applied optics

Cascaded on-chip phonon shield for membrane microresonators

Zhenqiang Ren,[1,2] Zongyang Li,[1,2] Doudou Wang,[1,2] Qiang Zhang,[1,2] and Yongmin Li[1,2,*]

[1]State Key Laboratory of Quantum Optics and Quantum Optics Devices, Institute of Opto-Electronics, Shanxi University, Taiyuan 030006, China
[2]Collaborative Innovation Center of Extreme Optics, Shanxi University, Taiyuan 030006, China
*Corresponding author: yongmin@sxu.edu.cn

Received 20 September 2018; revised 6 November 2018; accepted 14 November 2018; posted 15 November 2018 (Doc. ID 346465); published 12 December 2018

We propose to suppress acoustic wave coupling between a Si_3N_4 membrane resonator and its support structure through cascaded low-frequency resonators fabricated on the silicon substrate of the membrane. The on-chip silicon resonators are designed to ensure that the frequencies of their oscillatory motion are well separated from the mechanical modes of the membrane resonator. Using optical interferometry, we characterize the displacement response of the membrane frame with the vibration isolation; mechanical isolation >30 dB from the mounting surface is achieved. Thus, we reliably fabricate Si_3N_4 membrane resonators with mechanical quality factors of around 2×10^6 at room temperature.

https://doi.org/10.1364/AO.57.010436

1. INTRODUCTION

In recent years, the optomechanical interaction between a light field and mechanical motion via radiation pressure has found increasing interest in the fields of quantum optics, quantum information, fundamental tests of macroscopic quantum physics [1,2], etc. Owing to their outstanding mechanical and optical properties, highly stressed silicon nitride (Si_3N_4) membranes have emerged as an attractive platform in quantum optomechanics [3,4]. Recently, significant progress has been made in work based on membrane resonators, such as cooling the mechanical motion of the membranes to near the ground state [5–7], observation of radiation pressure shot noise [8], preparing optical squeezing states [9–12], probing deformed commutators with macroscopic harmonic oscillators [13], and investigating multimode four-wave mixing in an unresolved sideband optomechanical system [14]. All of these experiments and studies require that the membrane oscillators possess a high mechanical quality factor.

The performance of a microresonator crucially depends on its quality factor, which characterizes the resonator's mechanical dissipation rate. Two different kinds of loss mechanism exist: internal loss caused by the resonator itself (surface loss, Akhiezer damping, thermoelastic loss, etc.), and external loss, which derives from phonon tunneling loss of the mechanical resonator to its supporting structure [15–26]. High quality factors ($Q > 10^7$) can be achieved by decreasing the internal loss, such as using an ultrathin and high-stress membrane [27], designing tethered membranes [27,28], including a phononic crystal on the membrane [29], or placing the resonator in a low-temperature environment [30]. In addition, several methods have been developed to isolate the tunneling loss: improving the clamping method [4], nodal suspension [17], designing a phononic crystal substrate [18,21,23], utilizing a recoil damping effect [25], incorporating a low-frequency oscillator shield [26], and employing destructive interference [31–33]. The phononic crystal shield design requires a periodic structure to isolate the vibration and performs well for high-frequency mechanical resonators. However, for low-frequency resonators, the periodic structure will be large, which prevents the use of a compact design as well as suffering from the low-frequency vibration of the whole structure. The approach of a low-frequency oscillator exploits the property of a second-order low-pass filter, which efficiently blocks high-frequency vibrations well beyond the frequency of the low-frequency resonator shield and can work well in the relatively low-frequency range.

In consideration of the compactness and fabrication complexity, we present a compact and concise design for a membrane resonator. To this end, a cascaded on-chip low-frequency resonator is fabricated directly on the silicon substrate of a Si_3N_4 membrane. The designed specific on-chip structure requires only one etching depth. To avoid acoustic wave coupling between the membrane and the oscillatory motion of the silicon substrate and improve the isolation effect, we carefully designed the configuration and size of the silicon substrate and keep its eigenvibration frequencies well shifted from the frequencies of the membrane resonator. Mechanical isolation higher than 30 dB is achieved; this results in mechanical quality factors of around 2 million at room temperature.

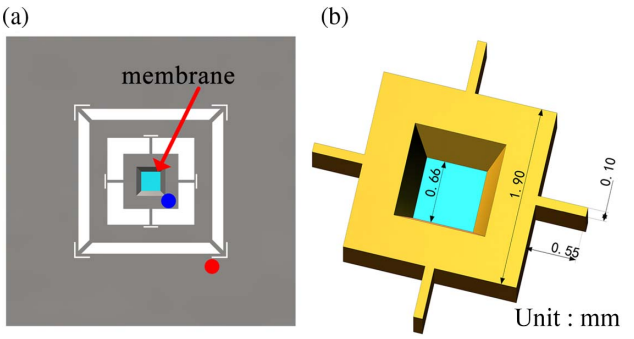

Fig. 1. (a) Chip; the blue and red spots denote the locations of the displacement response measurements given in Fig. 3. (b) Membrane frame.

2. DESIGN OF THE MEMBRANE MICRORESONATOR

A schematic diagram of the device is given in Fig. 1(a). The outer frame of the chip, which has an area of 10 mm × 10 mm and a thickness of 0.2 mm, is clamped at the corners to a piezoelectric actuator. The Si_3N_4 membrane, length 660 μm, is located in the center of a membrane frame with a side length of 1.7 mm, as shown in Fig. 1(b). The membrane frame is supported at four points by flexural and torsional springs of width 100 μm to form a low-frequency resonator. To further suppress the vibration, another on-chip low-frequency resonator is constructed just outside the membrane frame. This frame is also supported at its corners by four flexural and torsional springs, of width 140 μm, to ensure that two sets of strings are well separated spatially. Here, the structure of the strings minimizes the oscillatory motion deformation of the low-frequency resonators during the displacement; this effectively reduces the coupling of the low-frequency resonators with the remaining parts of the chip [25].

Figure 2 shows the modal shapes of the lowest-frequency resonances of the chip frame, determined using finite-element analysis. The lowest resonance frequency of the middle frame of the chip, which forms the outer low-frequency resonator, is 34 kHz [Fig. 2(a)]. The lowest resonance frequency of the inner frame (membrane frame) of the chip, which forms the inner low-frequency resonator, is 120 kHz [Fig. 2(b)]. By cascading the outer and the inner low-frequency resonator, the acoustic wave coupling between the membrane resonator and its support structure at the membrane's resonance frequency can be suppressed effectively at the frequency range much larger than the resonance frequency of the low-frequency resonators. In this way, the mechanical quality factor of the membrane can be enhanced.

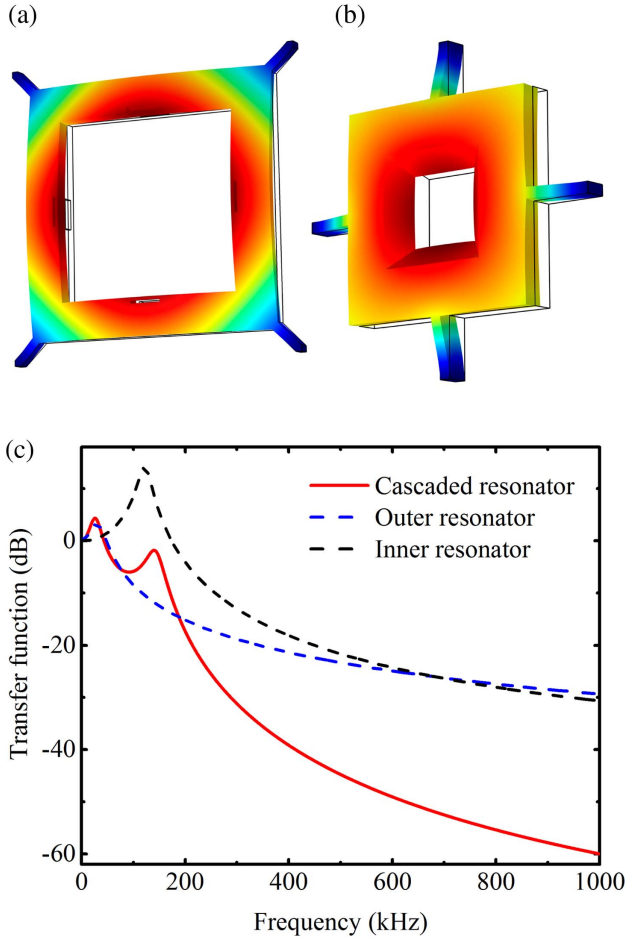

Fig. 2. (a) Modal shapes of the outer low-frequency oscillator at 34 kHz. (b) Modal shapes of the inner low-frequency oscillator at 120 kHz. (c) Theoretical mechanical transfer function of the device. The blue and black dashed lines denote the mass-on-spring modes of the inner and outer low-frequency resonators, respectively. The red line is the overall transfer function of the cascaded resonators.

Our coupled oscillator system can be approximated by a coupled mass-spring model. The coupled equations representing the mechanical motions are given by

$$m_1\ddot{x}_1 = -\gamma_1(\dot{x}_1 - \dot{y}) - k_1(x_1 - y) - k_2(x_1 - x_2), \quad (1)$$

$$m_2\ddot{x}_2 = -\gamma_2(\dot{x}_2 - \dot{x}_1) - k_2(x_2 - x_1), \quad (2)$$

where m_1 and m_2 are the effective mass of the outer and inner low-frequency resonators, respectively. $x_1(t)$ and $x_2(t)$ are their displacements, $k_1 = m_1\omega_1^2$ and $k_2 = m_2\omega_2^2$ are their spring constants, γ_1 and γ_2 are the intrinsic dissipation of the resonators, and $y(t)$ is the movement of the chip's outer frame.

Equations (1) and (2) can be solved to obtain the mechanical transfer function as follows:

$$T(\omega) = \frac{|x_2(\omega)|^2}{|y(\omega)|^2} = \left|\frac{k_1 - i\omega\gamma_1}{(k_2 - i\omega\gamma_2 - m_2\omega^2)(k_1 + k_2 - i\omega\gamma_1 - m_1\omega^2)/(k_2 - i\omega\gamma_2) - k_2}\right|^2. \quad (3)$$

Figure 2(c) is a plot of the simulated mechanical transfer function of the on-chip cascaded resonators. Both the outer and inner resonators act as mechanical low-pass filters, which

effectively isolate high-frequency vibrations in the range $\omega \gg \omega_{\text{outer}}$. Owing to the two cascaded low-pass filters, the overall isolation effect is better than would be obtained using only one low-pass filter.

Notably, although the cascaded low-frequency resonator can significantly suppress the coupling of the high-frequency acoustic waves, the isolation effect would be reduced in the frequency regime around the intrinsic oscillatory motions of the silicon frame. If the resonant frequencies of the membrane resonator are located close to these oscillatory frequencies of the chip frame, the membrane modes will couple to the chip frame modes and severely degrade the mechanical quality factor of the membrane [16].

The frequencies of the oscillatory motions of the silicon frame depend mainly on its size and geometrical configuration. To tune the frequencies of the chip frame away from the vibration modes of the membrane, we carefully designed the silicon frame, especially the geometric parameters of the grooves and the strings and their location in the chip frame.

3. MEASUREMENT RESULTS

To fabricate the device, a 50 nm thick Si_3N_4 film with 0.9 GPa tensile stress is grown by low-pressure chemical vapor deposition on a 200 μm thick silicon wafer. Further fabrication of the pattern on the device is implemented using standard microelectromechanical system technology [23]. The concise design of the on-chip structure, plus the requirement of only a uniform etching depth, make the device straightforward to realize. To characterize the vibration isolation effect of the cascaded phonon shield structure, the chip frame is clamped to a piezoelectric actuator at four corners and actuated using the output signal from a network analyzer. The displacement spectra of the device are extracted using an optical interferometer. More precisely, a single-frequency laser operating at 1064 nm shines on the sample, and the resulting backreflected beam is detected by a homodyne detector. The relative phase between the signal and the local oscillator is controlled to be $\pi/2$ to measure the phase information of the signal, which is fed into the network analyzer.

Figure 3 illustrates the measured mechanical response of the cascaded phonon shield in the low-frequency and high-frequency ranges, where the red curve (A) and blue curve (B) represent the measurement outcomes at the corresponding red and blue points marked in Fig. 1(a). The two lowest-resonance peaks simulated in Fig. 2(c) don't apparently appear in the measured displacements in Fig. 3 (marked I and II). We attribute this to the low Q values of the shield; in this case, the noisy background overwhelms the relatively weak and broad resonance peaks. In the low-frequency range, i.e., frequencies less than 150 kHz, the effect of the phonon tunneling isolation is not apparent. A significant vibration isolation, as high as 30 dB, is observed for frequencies higher than 250 kHz. Three peaks (marked III, IV, and V) are clearly observed around 260, 352, and 478 kHz, which represent the high-order oscillation modes of the chip frame and agree with the simulation results using finite-element analysis. As mentioned, the chip frame is carefully designed to ensure that these oscillation modes are separate from the membrane modes; otherwise, the

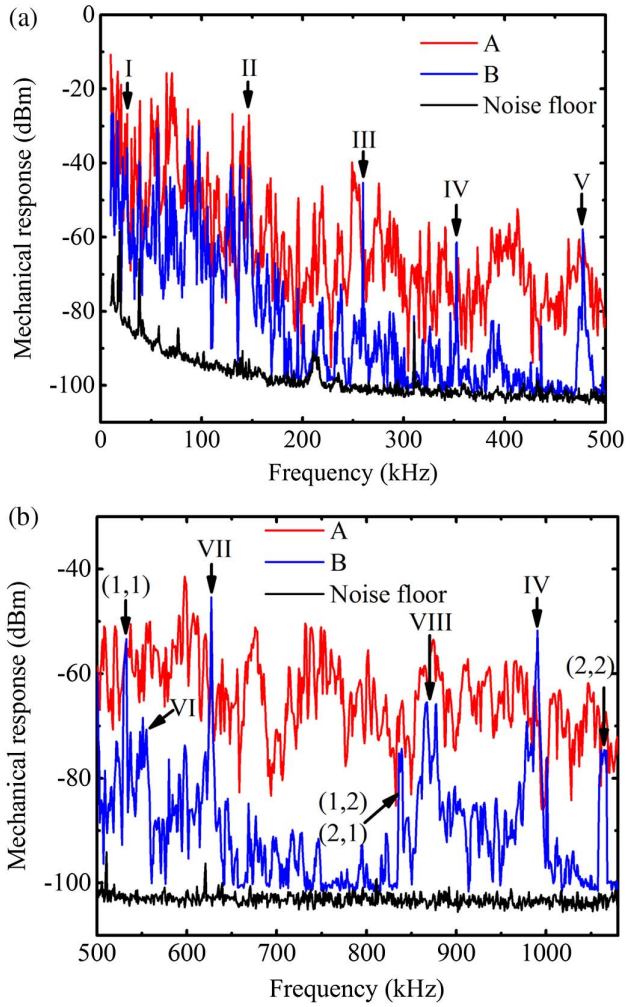

Fig. 3. Mechanical response spectra of the device: (a) 0–500 kHz; (b) 500–1200 kHz. A, displacement power spectra of the chip frame at the red point shown in Fig. 1(a). B, displacement power spectra of the chip frame at the blue point shown in Fig. 1(a). The black line denotes the noise floor of the homodyne detector.

oscillation modes would be detrimental to the mechanical quality factor of the membrane resonator.

In the high-frequency range, i.e., frequencies above 500 kHz, strong vibration isolation higher than 30 dB is achieved, as shown in Fig. 3(b). Four membrane modes, (1, 1), (1, 2), (2, 1), and (2, 2), at 529, 836, and 1058 kHz, are clearly observed. Notably, four high-order oscillation modes of the chip frame (VI, VII, VIII, and IV) at 550, 627, 870, and 990 kHz also exist in this frequency range, which agree with the simulation; however, they do not overlap the membrane modes except the oscillation modes of the chip frame around 550 kHz.

We measured the mechanical quality factor of the Si_3N_4 membrane using the mechanical ringdown technique. The chip was put in a vacuum chamber with a vacuum pressure of 10^{-6} mbar at room temperature. The mechanical quality factor is defined as $Q_m = 2\pi f\tau$, where τ is the ringdown time of mechanical vibration energy and f is the resonance frequency of the membrane modes. A typical result is shown in Fig. 4, where the black and red curves represent the measured data

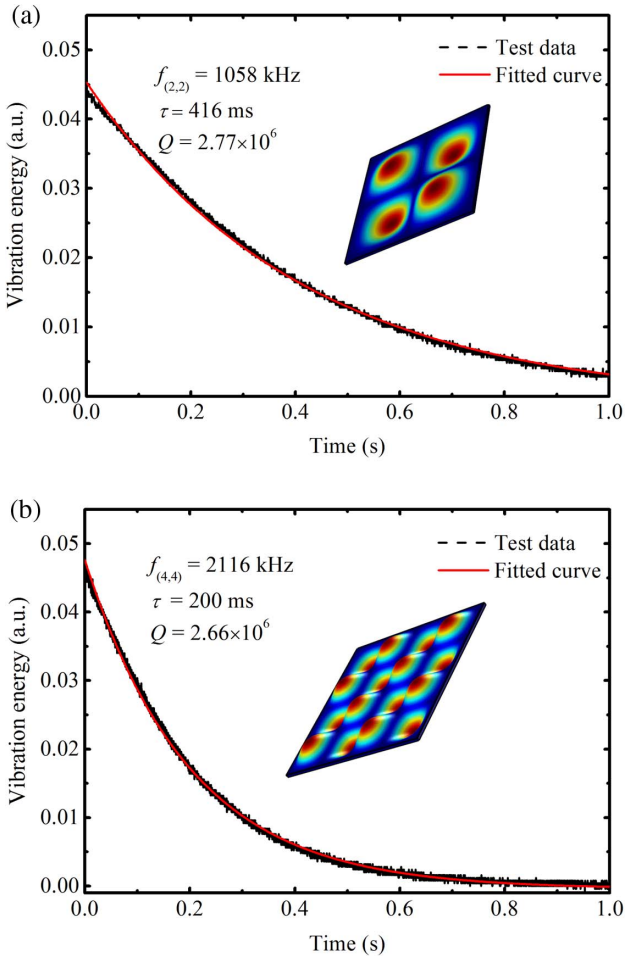

Fig. 4. Mechanical ringdown measurement of the quality factors: (a) membrane mode (2, 2); (b) membrane mode (4, 4).

and exponential curve fitting, respectively. We can see that the ringdown results agree well with the exponential decay curve. A long ringdown time, of hundreds of milliseconds, is observed. The evaluated Q values of the (2, 2) and (4, 4) modes are 2.77×10^6 and 2.66×10^6, respectively. The quality factors of five other devices that are without any obvious physical defects were also tested. The observed Q values distribute from 1 million to 3 million. In contrast, the test on 10 devices without the shield structure showed that Q values are distributed from 10^4 to 10^5, with the highest quality factor of 400,000. The above results verify the vibration isolation effect of our cascaded phonon shield.

We also measured the mechanical quality factors of the fundamental, (1, 2), and (2, 1) modes. Both the (1, 2) and (2, 1) modes have mechanical quality factors of around 1 million. However, the fundamental mode presents a relatively low Q factor of 4.6×10^5. The dissipation mechanism is attributed to the coupling of the fundamental mode to the oscillatory motion of the silicon frame. As shown in Fig. 3(b), a number of distinct resonances are located around the fundamental mode of the membrane. In future experiments, we will employ the (2, 2) mode and higher-order modes, which have relatively high resonance frequencies, above 1 MHz; therefore, no special measures are taken to suppress the dissipation of these low-order modes.

4. DISCUSSION AND CONCLUSION

In conclusion, we have provided a compact and concise design for a membrane resonator, using a cascaded on-chip silicon resonator, to suppress phonon tunneling loss efficiently. Based on this method, Si_3N_4 membrane microresonators with a mechanical quality factor around 2×10^6 at room temperature were reliably fabricated. The Q factor of the (4, 4) mode nearly satisfies the benchmark of ground-state cooling using the radiation pressure force at room temperature: $Q_m \times f > k_B T_{\text{room}}/h$, where k_B is the Boltzmann constant and h is the Planck constant. This regime is necessary for a number of optomechanical experiments operating in the quantum domain to be conducted [27,29]. To rigorously satisfy the benchmark, higher-order modes, such as the (5, 5) mode, can be used. Alternatively, we can operate the device at −20°C simply by using an ordinary Peltier cooler. In our future work, we will cool the membrane mode of the device close to the ground state in the unresolved sideband regime [34] and attempt to produce nonclassical states of the mechanical modes [35].

Funding. National Key R&D Program of China (2016YFA0301403); National Natural Science Foundation of China (NSFC) (11774209, 61378010); Shanxi 1331KSC; Program for the Outstanding Innovative Teams of Higher Learning Institutions of Shanxi.

REFERENCES

1. T. J. Kippenberg and K. J. Vahala, "Cavity optomechanics: back-action at the mesoscale," Science **321**, 1172–1176 (2008).
2. M. Aspelmeyer, T. J. Kippenberg, and F. Marquardt, "Cavity optomechanics," Rev. Mod. Phys. **86**, 1391–1452 (2014).
3. J. D. Thompson, B. M. Zwickl, A. M. Jayich, F. Marquardt, S. M. Girvin, and J. G. E. Harris, "Strong dispersive coupling of a high-finesse cavity to a micromechanical membrane," Nature **452**, 72–75 (2008).
4. D. J. Wilson, C. A. Regal, S. B. Papp, and H. J. Kimble, "Cavity optomechanics with stoichiometric SiN films," Phys. Rev. Lett. **103**, 207204 (2009).
5. M. Karuza, C. Molinelli, M. Galassi, C. Biancofiore, R. Natali, P. Tombesi, G. D. Giuseppe, and D. Vitali, "Optomechanical sideband cooling of a thin membrane within a cavity," New J. Phys. **14**, 095015 (2012).
6. M. Underwood, D. Mason, D. Lee, H. Xu, L. Jiang, A. B. Shkarin, K. Børkje, S. M. Girvin, and J. G. E. Harris, "Measurement of the motional sidebands of a nanogram-scale oscillator in the quantum regime," Phys. Rev. A **92**, 061801 (2015).
7. R. W. Peterson, T. P. Purdy, N. S. Kampel, R. W. Andrews, P.-L. Yu, K. W. Lehnert, and C. A. Regal, "Laser cooling of a micromechanical membrane to the quantum backaction limit," Phys. Rev. Lett. **116**, 063601 (2016).
8. T. P. Purdy, R. W. Peterson, and C. A. Regal, "Observation of radiation pressure shot noise on a macroscopic object," Science **339**, 801–804 (2013).
9. A. H. Safavi-Naeini, S. Gröblacher, J. T. Hill, J. Chan, M. Aspelmeyer, and O. Painter, "Squeezed light from a silicon micromechanical resonator," Nature **500**, 185–189 (2013).
10. T. P. Purdy, P.-L. Yu, R. W. Peterson, N. S. Kampel, and C. A. Regal, "Strong optomechanical squeezing of light," Phys. Rev. X **3**, 031012 (2013).

11. F. Lecocq, J. B. Clark, R. W. Simmonds, J. Aumentado, and J. D. Teufel, "Quantum nondemolition measurement of a nonclassical state of a massive object," Phys. Rev. X **5**, 041037 (2015).
12. W. H. P. Nielsen, Y. Tsaturyan, C. B. Møller, E. S. Polzik, and A. Schliesser, "Multimode optomechanical system in the quantum regime," Proc. Natl. Acad. Sci. U.S.A. **114**, 62–66 (2017).
13. M. Bawaj, C. Biancofiore, M. Bonaldi, F. Bonfigli, A. Borrielli, G. D. Giuseppe, L. Marconi, F. Marino, R. Natali, A. Pontin, G. A. Prodi, E. Serra, D. Vitali, and F. Marina, "Probing deformed commutators with macroscopic harmonic oscillators," Nat. Commun. **6**, 7503 (2015).
14. Z. Y. Li, X. You, Y. M. Li, Y. C. Liu, and K. C. Peng, "Multimode four-wave mixing in an unresolved sideband optomechanical system," Phys. Rev. A **97**, 033806 (2018).
15. I. Wilson-Rae, R. A. Barton, S. S. Verbridge, D. R. Southworth, B. Ilic, H. G. Craighead, and J. M. Parpia, "High-Q nanomechanics via destructive interference of elastic waves," Phys. Rev. Lett. **106**, 047205 (2011).
16. A. Jöckel, M. T. Rakher, M. Korppi, S. Camerer, D. Hunger, M. Mader, and P. Treutlein, "Spectroscopy of mechanical dissipation in micromechanical membranes," Appl. Phys. Lett. **99**, 143109 (2011).
17. G. D. Cole, I. Wilson-Rae, K. Werbach, M. R. Vanner, and M. Aspelmeyer, "Phonon-tunnelling dissipation in mechanical resonators," Nat. Commun. **2**, 231 (2011).
18. A. H. Safavi-Naeini and O. Painter, "Design of optomechanical cavities and waveguides on a simultaneous bandgap phononic-photonic crystal slab," Opt. Express **18**, 14926–14943 (2010).
19. K. K. Ni, R. Norte, D. J. Wilson, J. D. Hood, D. E. Chang, O. Painter, and H. J. Kimble, "Enhancement of mechanical Q factors by optical trapping," Phys. Rev. Lett. **108**, 214302 (2012).
20. P.-L. Yu, T. P. Purdy, and C. A. Regal, "Control of material damping in high-Q membrane microresonators," Phys. Rev. Lett. **108**, 083603 (2012).
21. Y. Tsaturyan, A. Barg, A. Simonsen, L. G. Villanueva, S. Schmid, A. Schliesser, and E. S. Polzik, "Demonstration of suppressed phonon tunneling losses in phononic bandgap shielded membrane resonators for high-Q optomechanics," Opt. Express **22**, 6810–6821 (2014).
22. S. Chakram, Y. S. Patil, L. Chang, and M. Vengalattore, "Dissipation in ultrahigh quality factor SiN membrane resonators," Phys. Rev. Lett. **112**, 127201 (2014).
23. P.-L. Yu, K. Cicak, N. S. Kampel, Y. Tsaturyan, T. P. Purdy, R. W. Simmonds, and C. A. Regal, "A phononic bandgap shield for high-Q membrane microresonators," Appl. Phys. Lett. **104**, 023510 (2014).
24. Z. Y. Li, Q. Zhang, X. You, Y. M. Li, and K. C. Peng, "Suppression of phonon tunneling losses by microfiber strings for high-Q membrane microresonators," Appl. Phys. Lett. **109**, 191903 (2016).
25. A. Borrielli, L. Marconi, F. Marin, F. Marino, B. Morana, G. Pandraud, A. Pontin, G. A. Prodi, P. M. Sarro, E. Serra, and M. Bonaldi, "Control of recoil losses in nanomechanical SiN membrane resonators," Phys. Rev. B **94**, 121403 (2016).
26. M. J. Weaver, B. Pepper, F. Luna, F. M. Buters, H. J. Eerkens, G. Welker, B. Perock, K. Heeck, S. de Man, and D. Bouwmeester, "Nested trampoline resonators for optomechanics," Appl. Phys. Lett. **108**, 033501 (2016).
27. R. A. Norte, J. P. Moura, and S. Gröblacher, "Mechanical resonators for quantum optomechanics experiments at room temperature," Phys. Rev. Lett. **116**, 147202 (2016).
28. C. Reinhardt, T. Müller, A. Bourassa, and J. C. Sankey, "Ultralow-noise SiN trampoline resonators for sensing and optomechanics," Phys. Rev. X **6**, 021001 (2016).
29. Y. Tsaturyan, A. Barg, E. S. Polzik, and A. Schliesser, "Ultra-coherent nanomechanical resonators via soft clamping and dissipation dilution," Nat. Nanotechnol. **12**, 776–783 (2017).
30. B. M. Zwickl, W. E. Shanks, A. M. Jayich, C. Yang, A. C. B. Jayich, J. D. Thompson, and J. G. E. Harris, "High quality mechanical and optical properties of commercial silicon nitride membranes," Appl. Phys. Lett. **92**, 103125 (2008).
31. X. Sun, J. Zheng, M. Poot, C. W. Wong, and H. X. Tang, "Femtogram doubly clamped nanomechanical resonators embedded in a high-Q two-dimensional photonic crystal nanocavity," Nano Lett. **12**, 2299–2305 (2012).
32. M. Zhang, G. Luiz, S. Shah, G. Wiederhecker, and M. Lipson, "Eliminating anchor loss in optomechanical resonators using elastic wave interference," Appl. Phys. Lett. **105**, 051904 (2014).
33. G. O. Luiz, R. S. Benevides, F. G. S. Santos, Y. A. V. Espinel, T. P. M. Alegre, and G. S. Wiederhecker, "Efficient anchor loss suppression in coupled near-field optomechanical resonators," Opt. Express **25**, 31347–31361 (2017).
34. D. J. Wilson, V. Sudhir, N. Piro, R. Schilling, A. Ghadimi, and T. J. Kippenberg, "Measurement-based control of a mechanical oscillator at its thermal decoherence rate," Nature **524**, 325–329 (2015).
35. X. You, Z. Y. Li, and Y. M. Li, "Strong quantum squeezing of mechanical resonator via parametric amplification and coherent feedback," Phys. Rev. A **96**, 063811 (2017).